Journal of the Meteorological Society of Japan, Vol. 76, No. 1, pp. 1–12, 1998

Role of Warming over the Tibetan Plateau in Early Onset of the Summer Monsoon over the Bay of Bengal and the South China Sea

By Hiroaki Ueda[1] and Tetsuzo Yasunari

Institute of Geoscience, University of Tsukuba, Ibaraki 305, Japan

(Manuscript received 10 March 1996, in revised form 9 September 1997)

Abstract

In this study we examine the mechanisms of the onset of the Southeast Asian monsoon (SEAM) over the Bay of Bengal and the South China Sea in terms of thermal contrast between the Tibetan Plateau and surrounding ocean based upon 5-day mean ECMWF circulation field data (1980–89) and 5-day mean GMS equivalent black body temperature (T_{BB}) data. The early onset of the SEAM is recognizable at Pentad 28 (May 16–20) with accelerated low-level monsoon westerlies followed by second enhancement of the monsoon activities in early June.

The warming over the Tibetan Plateau from spring to summer is found in the 200–500 hPa thickness data on about 15-day intervals. Of importance is the observational evidence that the warming phase over the Tibetan Plateau around mid-May is concurrent with the early onset of the SEAM. Thus, the thermal contrast between the Tibetan Plateau and the adjacent ocean is likely to induce the acceleration and eastward extension of the low-level monsoon flow, causing the abrupt commencement of the SEAM including onset of the South China Sea monsoon (SCSM). This relationship between low-level wind over the key region (10°–20°N, 80°–120°E) and 200–500 hPa thickness over the Tibetan Plateau is also confirmed based on the correlation analysis in the interannual variabilities.

An influence for the mid-latitude atmosphere, stationary Rossby waves are generated over the South China Sea and propagate in a northeastward direction toward Japan because of the cyclonic vorticity and the tropical heat source associated with the onset of the SCSM. As a result of this wave propagation, a high pressure anomaly appears over Japan, which is consistent with a singularity of clear skies around Japan in mid-May (Kawamura and Tian, 1992).

1. Introduction

The term "monsoon" is defined as an annual reversal of seasonal dominated steady wind direction of more than 120 degrees between summer and winter (Khromov, 1957). With respect to the seasonal evolution of a large-scale Asian/Australian monsoon, Murakami and Nakazawa (1985) showed that the transition of a summer monsoon from the Southern Hemisphere to the Northern Hemisphere is closely associated with a symmetric equatorial heat source over the Sumatra-Borneo-New Guinea region. Matsumoto (1992) divided the Asian and Australian monsoon into eleven subseasons based upon the observed abrupt seasonal changes. These abrupt changes were partly recognizable using a global circulation model simulation (Lau and Yang, 1996). Nakazawa (1992) showed that this phenomena occurs on intraseasonal time scales that are phase-locked with the seasonal cycle. Tanaka (1992) also indicated that the rapid northward migration of cloud bands observed by GMS in East Asia have similar characteristics.

According to Khromov's definition, broad tropical and subtropical regions in Asia/Australia are characterized as a single, uniform monsoon climate system. However, Murakami and Matsumoto (1994) subdivided the monsoon regions into several parts based on annual differences in OLR of more than 60 Wm^{-2} *i.e.*, a reversal between wet and dry season. Their result indicates that the western North Pacific monsoon (WNPM) between 120°–150°E from 10° to 20°N is one of the important monsoon domains separated from the Southeast Asia monsoon (SEAM). A classical idea of the broad monsoon circulation is a sort of large-scale land and sea breeze induced by seasonal differen-

1 Corresponding author: Research Fellow of the Japan Society for Promotion of Science H. Ueda, Institute of Geoscience, University of Tsukuba, 1-1-1 Tennodai, Tsukuba, Ibaraki, 305, Japan. E-mail: ueda@etesia.geo.tsukuba.ac.jp

tial heating between the Eurasian continent and the adjacent oceans. Interestingly, the WNPM exhibits drastic annual variations despite having much less continental-scale heating when compared with that of the SEAM. Ueda *et al.* (1995) showed that an abrupt northeastward shift of the enhanced convection appears over the subtropical western North Pacific around 25°N, 150°E during late July (convection jump) with eastward extension of the low-level monsoon westerlies, which results in the withdrawal of the *Baiu* season around Japan. Furthermore, the mechanism of the seasonal evolution over the western Pacific from middle June to late July is closely related to the air-sea interaction of the area (Ueda and Yasunari, 1996).

It is important to note that the South China Sea monsoon (SCSM) appears to show different characteristics from both the SEAM and the WNPM (Murakami and Matsumoto, 1994). The annual OLR amplitude of the SCSM along 15°N shows a minimum (50 Wm^{-2}) in contrast with a much larger value of 80 Wm^{-2} over the Bay of Bengal and the Philippines. Moreover, the influence of land-sea thermal contrast may not be negligible over the South China Sea due to its location near the Asian continent. Quite recently, So and Chan (1997) indicated that a north-south temperature gradient between South China and northern Australia play an important role for the establishment of the summer monsoon over South China around Hong Kong. Chen and Chen (1995) revealed that the onset and life cycle of the SCSM over the South China Sea is regulated by the alternation of the northward-migrating 30–60 day monsoon trough and ridge. Furthermore, this intraseasonal mode is coupled with a eastward-propagating 30–60 day mode of the global divergent circulation (Chen *et al.*, 1988). In relation to the intraseasonal oscillation, Chen and Weng (1996) showed that the 30–60 day mode has a profound impact on the occurrence frequency and westward propagation of equatorial waves. However, the climatological features of the seasonal evolution of the SCSM has not been revealed in detail and its mechanism is usually explained in terms of intraseasonal variations. Therefore, the main objectives of this paper are 1) to reveal climatological features of the onset and the life cycle of the SEAM, especially over the South China Sea and the Bay of Bengal, and 2) to examine the roles of the continent-ocean temperature gradient for the seasonal evolution of the SEAM, including the role played by warming of the Tibetan Plateau.

In Section 2 we document the data. In Section 3 we describe the seasonal changes of the convective activities and wind field over the South China Sea to the Bay of Bengal, and we reveal its horizontal structure during the onset phase. Section 4 examines the temperature field over the Tibetan Plateau and its relation to the evolution of the SCSM. The conclusions are given in Section 5.

2. Data

The data used in this study are pentad (5 day) mean-infrared-equivalent-black-body-temperature (T_{BB}) data observed from Geostationary Meteorological Satellite (GMS) for the period January 1980 to August 1994. The original T_{BB} is three-hourly and has a one degree, longitude-latitude grid resolution covering from 80° E to 180°E between 60°N and 60°S. The T_{BB} is considered to be a useful index of large-scale convective activity similar to the OLR data over the tropical and the subtropical regions. The twice-daily (0000 and 1200 UTC) objectively analyzed data on each 2.5° × 2.5° grid provided by the ECMWF (European Center for Medium-range Weather Forecast) 4-dimensional data assimilation (4DDA) system are used for the period January 1980 to December 1989. The data used are 5-day mean zonal and meridional wind components (u, v), the geopotential height (z) and temperature (T) at 4 pressure levels (1000, 850, 500, 200 hPa) on each grid point. We also used the daily precipitation data at Sanhu Island (16.53°N, 116.62°E) over the South China Sea for the period from 1977 to 1991 (National Climatic Data Center, 1994).

3. Convection and circulation fields

In this section, we describe large-scale convection and wind fields, focusing on the onset phase of a summer monsoon around Southeast Asia, especially over the Bay of Bengal and the South China Sea. Figure 1 shows latitude-time sections of 15-year mean T_{BB} and 10-year mean wind fields at 850 hPa averaged (a) between 85°E and 95°E, and (b) between 110°E and 120°E from January to December. The arrow indicates the horizontal wind direction, and shading denotes areas of T_{BB} of less than 270 K showing active convection in the tropics.

In the upper panel of the figure corresponding to the Bay of Bengal, an area of active convection is seen throughout of the year between 10°S and 5°N. During mid-May to early June, the enhanced convection continuously moves northward from 10°N to 20°N accompanied with commencement of westerly wind, which indicates the onset of the summer monsoon. Consecutively, the convection around 15°N reaches the peak phase in mid-June, and this active convection and strong westerlies persist until mid-September, then gradually retreat southward up to 10°N until the end of the year.

The lower panel of this figure shows the seasonal variation over the South China Sea. In the Southern Hemisphere the active convective region disappears during the Northern Hemisphere summer season, and begins to spread southward to around 5°S during September and reaches the most active phase

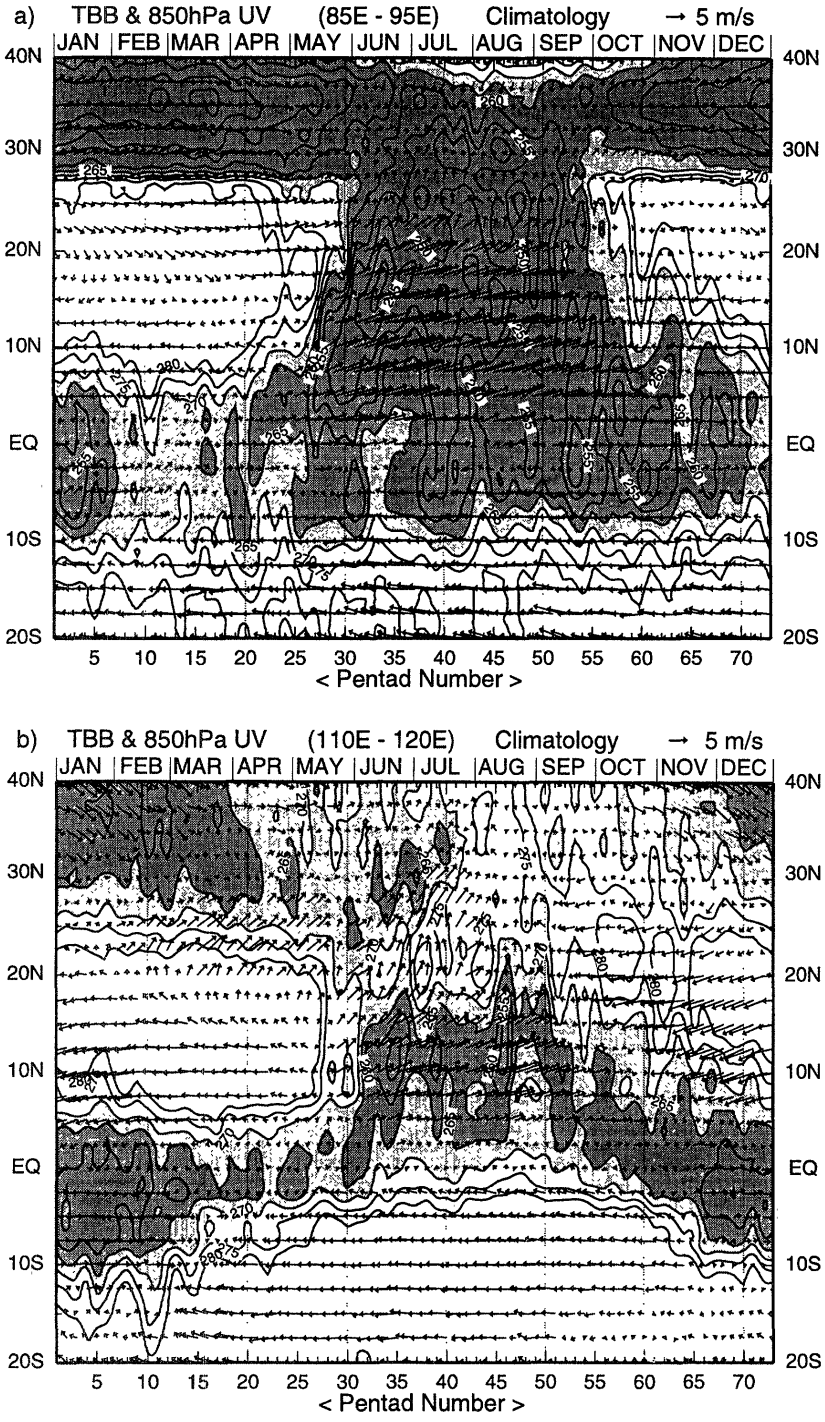

Fig. 1. Latitude-time sections of 15-year (1980–1994) mean T_{BB} and 10-year (1980–1989) mean 850 hPa wind averaged over between a) 85° and 95°E, and b) 110° and 120°E. Arrows indicate wind speed and direction (unit vector 5 ms^{-1}). T_{BB} contour intervals are for 5 K, and dark shading denotes areas with less than 265 K, while light shading between 265 and 270 K.

around January. Subsequently, this active convection area gradually shifts northward. As for the wind field, easterlies prevail throughout the season except for the period of the appearance of the most active convection between December and February. On the other hand, the seasonal transitions of circulation fields in the Northern Hemisphere between the equator and 20°N exhibit quite a different character compared with that of the Southern Hemisphere. The alternations of wind direction are distinct around mid-May (Pentad 28). Easterlies are dominant between November and early May, while the replacement of southwesterlies is clearly seen around mid-May. Hirasawa *et al.* (1995) showed

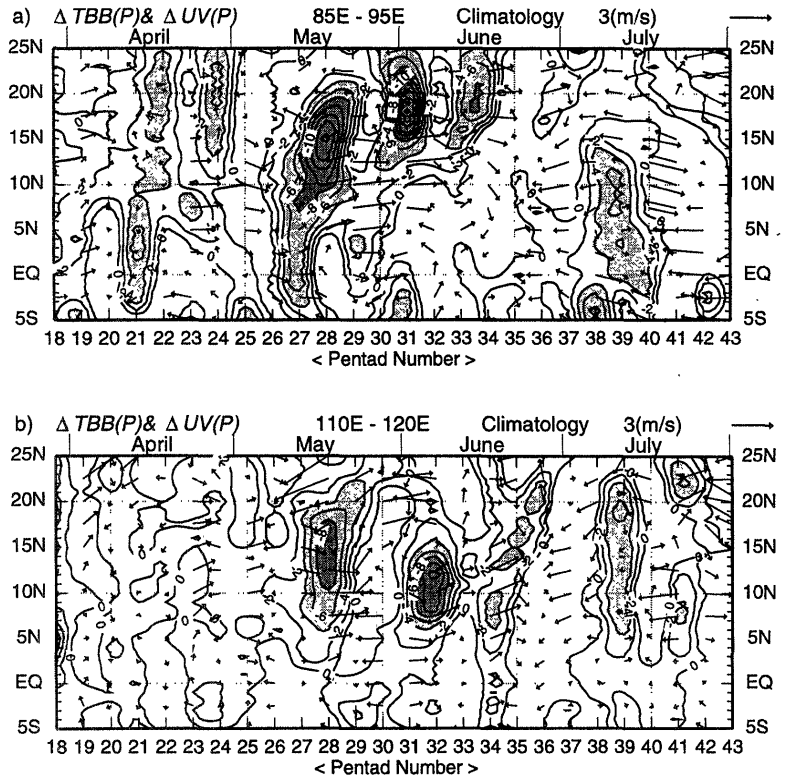

Fig. 2. Latitude -time section of the 15-year (1980–1994) averaged differential T_{BB} ($\Delta T_{BB}(P) = T_{BB}(P) - T_{BB}(P-1)$) and 10-year (1980–1989) mean differential wind at 850 hPa ($\Delta UV(P) = UV(P) - UV(P-1)$) along a) 85°–95°E, and b) 110°–120°E, where P is Pentad number. The reference vector is denoted in upper right of this figure. Light shading is T_{BB} between −4 and −8 K, while dark shading is less than −8 K.

that the abrupt seasonal change of the East Asian cloud band in mid-May or late May is closely associated with the enhancement of the low-level southwesterly wind. After this change of wind direction, the low-level monsoon westerlies accelerate until August, then the strong westerlies gradually become weak southward of 20°N and are further replaced by easterlies during September and October. The most active convection (T_{BB} of less than 265 K) can be seen in the beginning of June (Pentad 31) which follows the abrupt change of the wind direction (Pentad 28) by about 15 days.

Figure 2 shows climatological mean differential T_{BB} and 850 hPa wind vector along a) 85°E–95°E and, b) 110°–120°E , defined by,

$$\Delta T_{BB}(P) = T_{BB}(P) - T_{BB}(P-1) \quad (1)$$

$$\Delta UV(P) = UV(P) - UV(P-1) \quad (2)$$

where UV is wind vector at 850 hPa and P is pentad number. These values are useful to examine the degree of the seasonal changes. Over the Bay of Bengal (Fig. 2a), remarkable T_{BB} differences are not recognizable before mid-May. On the other hand, drastic seasonal change can be seen at Pentad 28 with acceleration of westerly wind, which indicates the commencement of the summer monsoon. This abrupt change at Pentad 28 is also recognizable over the South China Sea (Fig. 2b). In addition, lower T_{BB} values are also found during early June with a westerly wind anomaly, which is considered to be associated with the appearance of the ITCZ over the tropical western Pacific found by Murakami and Matsumoto (1994). In this manner, the abrupt seasonal changes are recognizable at Pentad 28 both over the Bay of Bengal and the South China Sea, indicating the early onset of the SEAM. However, intensity of the convective activities over the South China Sea is weaker than that of the Bay of Bengal. Therefore, the onset date of the SCSM derived from the satellite should be ascertained by local precipitation data, because the monsoon onset is regarded as a commencement of a rainfall. Figure 3 depicts seasonal changes of climatological mean precipitation for the period from 1977 to 1991 over the Sanhu Island (16.53°N, 116.62°E), a representative station over the South China Sea. Pentad mean value is calculated based on the daily precipitation data. In this figure, two maximums are observed in both June and September. A noticeable feature is that pentad mean precipitation in excess of 4 mm is seen at Pentad 28, which is consistent with the onset date obtained in T_{BB} data. This result supports the the-

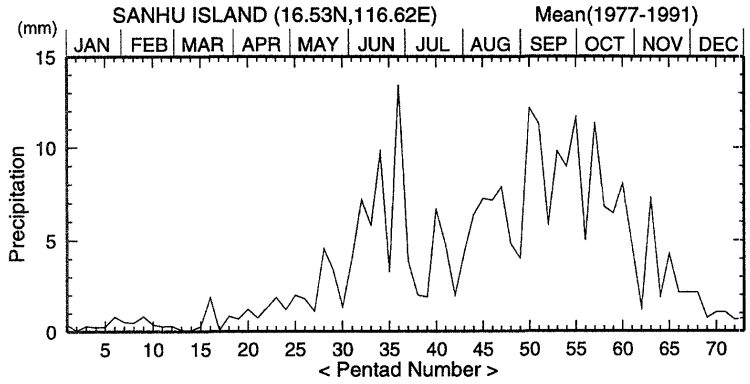

Fig. 3. Seasonal changes of pentad mean precipitation at Sanhu Island (16.53°N, 116.62°E) averaged over the period from 1977 to 1991.

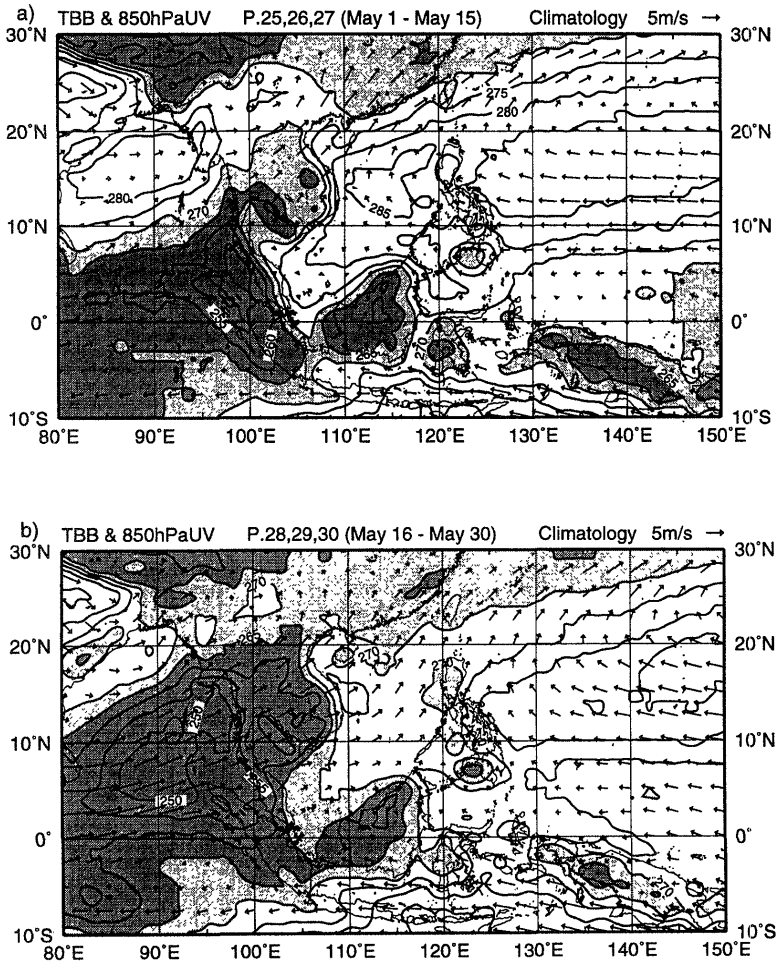

Fig. 4. 10-year averaged 850 hPa wind (unit vector 5ms^{-1}) and 15-year averaged T_{BB} (5 K intervals) fields (a) Pentad 25,26,27 (May 1–15), and (b) Pentad 28, 29 ,30 (May 16–30). Scale vector is shown at the upper-right of each figure. Dark shading denotes areas with T_{BB} less than 265 K, while light shading indicates T_{BB} between 265 and 270 K.

ory that the onset of the SCSM occurred at Pentad 28, although the values of T_{BB} are relatively large compared with those of over the Bay of Bengal.

In order to reveal the horizontal structure of the abrupt change in mid-May, the spatial distribution of 15-day mean T_{BB} and 850 hPa wind are shown in Fig. 4. Prior to the onset of the SEAM (upper panel), strong easterlies are dominant between 5°N and 20°N east of the Philippine Islands. These easterlies penetrate up to the South China

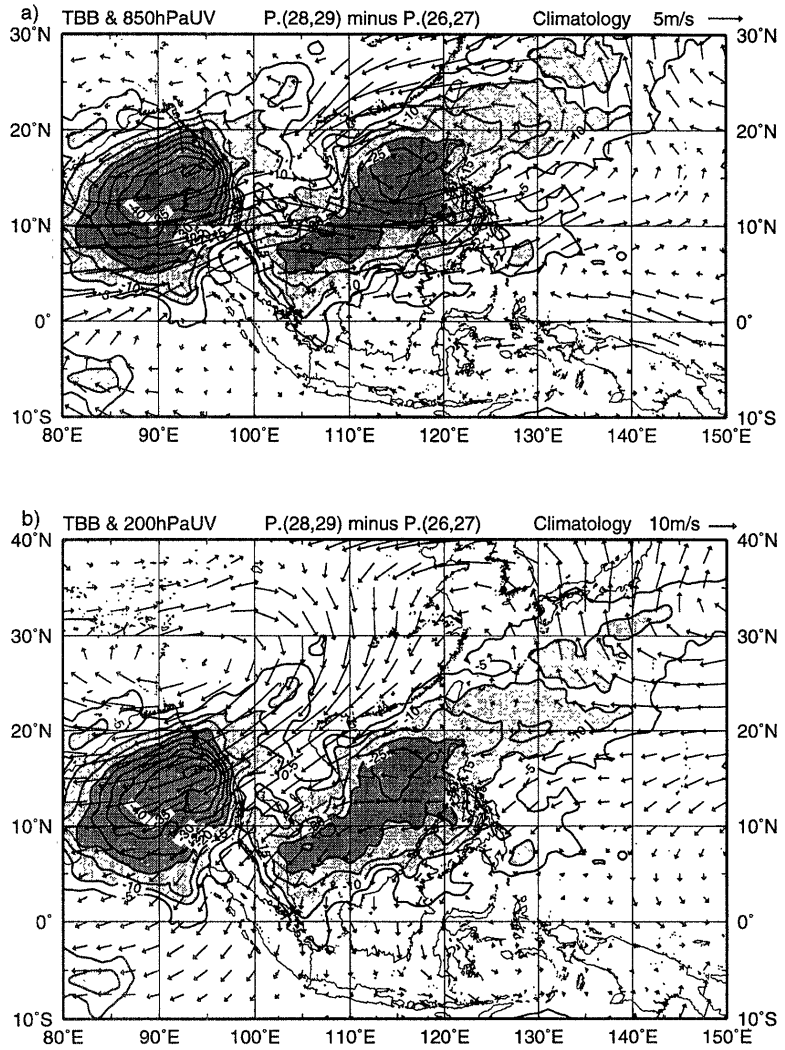

Fig. 5. Difference in 15-year averaged (1980–1994) T_{BB} and 10-year averaged (1980–1989) wind fields between Pentad (28,29) minus Pentad (26,27) for a) 850 hPa, and b) 200 hPa. The unit vector is denoted at the upper right corner. The contour interval is 5 K, with shading (dark shading) indicating regions of less than −10 K (−20 K)

Sea around 110°E where low-level monsoon westerlies merge with the easterlies. Eventually, southwesterlies are formed directed toward South China and Japan. The above features are consistent with the case study of the SCSM during 1979 (Chen and Chen, 1995). In this period, the active convection (T_{BB} of less than 250 K) is located over the maritime continent *i.e.*, Malaysian Peninsula, the Borneo Islands and the New Guinea Islands due to the active diurnal variation of convection (M. Murakami, 1983; Chen and Takahashi, 1994). The value of T_{BB} over the South China Sea and the Bay of Bengal north of 10°N is about 280 K indicating inactive convection. On the other hand, the convection over the Bay of Bengal south of 10°N is relatively active where monsoon westerlies are dominant.

Figure 4b depicts the features of the onset phase of the SEAM during Pentad 28–30 (May 16–30). Outstanding changes can be found in the wind fields over the South China Sea (5°N–20°N, 110°E–120°E). The easterlies seen in the previous period are replaced by the monsoon southwesterlies. It is important to note that the convective activities west of 110°E over Indochina to the Bay of Bengal are enhanced compared with that of the pre-onset phase with acceleration of low-level monsoon southwesterlies. Recently, Matsumoto (1997) showed that the full onset of the summer monsoon circulation over the Bay of Bengal, Indochina and the South China Sea begins in mid-May, causing active convection over there. Interestingly, the Indian monsoon is not established yet during this period; the convection is not active and northwesterlies are dominant over the Indian continent.

Figure 5 shows the difference of T_{BB} and wind fields a) 850 hPa, b) 200 hPa between the onset

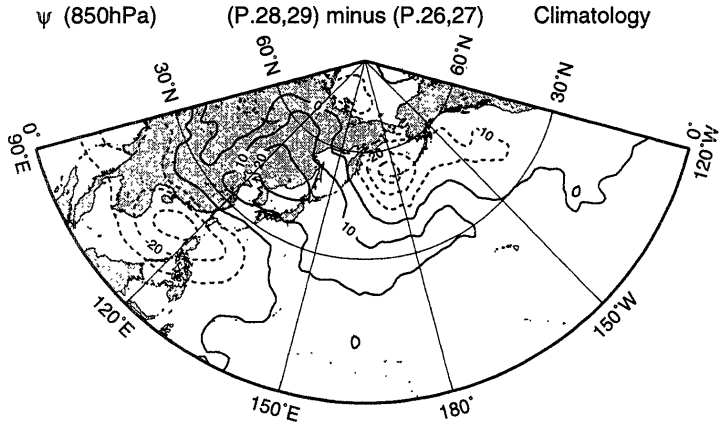

Fig. 6. Differences in the climatological mean (1980–89) geostrophic streamfunction for Pentads (28, 29) minus Pentads (26, 27) at 850 hPa. The contour intervals is 10 gpm.

phase (Pentad 28–29) minus the previous period (Pentad 26–27). Negative T_{BB} values (shaded area) indicate enhanced convection. In the upper panel of this figure, lower T_{BB} is located over the South China Sea, where a cyclonic wind anomaly is obvious. Krishnamurti *et al.* (1981) described the appearance of the "onset vortex" during the shift of northwesterlies to southwesterlies over the Arabian Sea. It is probable that the aforementioned cyclonic wind anomaly over the South China Sea is similar to the onset vortex over the Arabian Sea. Quite recently, Wang and Xu (1996) also showed that active convective anomalies shift northwestward from the northern Philippines to the South China Sea with low-level cyclonic circulation anomalies during Pentad 27 to 28, which are closely linked to the Northern Hemisphere summer monsoon singularities. Moreover, lower T_{BB} values are found over the Bay of Bengal where a westerly anomaly is evident, which indicates the strengthening of monsoon activities. As for the 200 hPa wind fields illustrated in the lower panel, an acceleration of easterly jet is obvious over the Bay of Bengal, which is connected with an anticyclonic wind anomaly over south of the Tibetan Plateau. This implies that the intensification of the Tibetan high induces the onset of the SEAM. Lau and Yang (1996) showed that the above abrupt change is accompanied by a rapid intensification of low-level westerlies and upper-level easterlies, and a corresponding northward shift of the ascending leg of the local meridional circulation. These results indicate that the onset of a SEAM is not induced by a local system like a subtropical western Pacific monsoon (Ueda and Yasunari, 1996), but is rather influenced by the large-scale forcing such as thermal contrast between the Eurasian continent and adjacent oceans, which will be argued in the next section.

To examine the influence of the abrupt change of circulation field at Pentad 28 upon the mid latitude atmosphere, geopotential height fields at 850 hPa are investigated. Fig. 6 represents the difference of quasi geostrophic stream function (Ψ) between Pentad 28, 29 minus Pentad 26, 27. The quasi geostrophic stream function is defined as follows:

$$\Psi = \Phi / f, \tag{3}$$

$$f = 2\omega \sin\theta, \tag{4}$$

where Φ is geopotential height, f is Coliolis parameter, ω is the earth's angular speed of rotation and θ is latitude, respectively. The geopotential difference pattern exhibits negative anomalies over the South China Sea, and positive anomalies over mid-latitudes around 30°–60°N, 120°–150°E, and negative anomalies appearing over the Aleutian Islands. The above patterns stretch northeastward from the South China Sea implying the propagation of stationary Rossby waves induced by tropical heat sources associated with the onset of the SCSM. The first negative anomalies correspond to both a cyclonic wind anomaly and a region of enhanced convection (see Fig. 5a). Kawamura and Tian (1992) showed that a singularity of clear skies appears around Japan at Pentad 29 based on the analysis of long-term weather data. This result agrees well with the positive geopotential anomaly over Japan as seen in Fig. 6.

The influence of tropical convection for the mid-latitude atmosphere during the summer season was investigated by Nitta (1986). He found north-south oscillation patterns between the western Pacific near 20°N and the middle latitudes around 35°N (called a "PJ pattern"). In terms of interannual variabilities, Nitta (1987) showed that stationary Rossby waves are generated over the Philippine Sea by active convection due to warm SST conditions and propagate

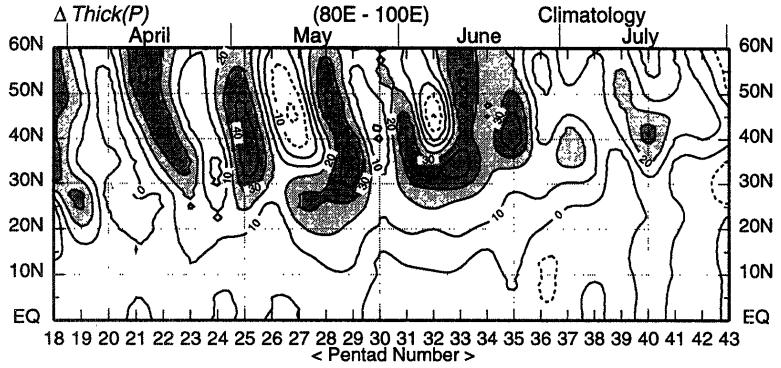

Fig. 7. Latitude-time sections of the degree of seasonal variation in 10-year averaged differential thickness ($\Delta Thick = Thick(P) - Thick(P-1)$), where $Thick(P)$ is height difference between 200 hPa minus 500 hPa averaged over 80°–100°E. The contour interval is 10 gpm. Dark shading denotes areas of $\Delta Thick$ greater than 30 gpm, while light shading indicates $\Delta Thick$ between 20 and 30 gpm.

northeastward during warm SST summers. In regard to the seasonal cycle, the northeastward propagation of stationary Rossby waves from the abrupt enhanced convective regions are identified by previous studies (Ueda *et al.*, 1995; Ueda and Yasunari, 1996; Ueda and Yasunari, 1997).

4. Temperature fields over the Tibetan Plateau

Since the Southeast Asia is near the continent, the atmospheric circulation over Southeast Asia might easily be affected by large-scale differential heating between the Eurasian continent and the adjacent ocean. The importance of the Tibetan Plateau as a heat source for the summer monsoon has been discussed by many authors (Gao *et al.*, 1981; Fu and Fletcher, 1985; Luo and Yanai, 1984; Murakami, 1987, 1993). Li and Yanai (1996) suggested that the onset of the low-level monsoon southwesterlies, which occur on the south side of the Tibetan Plateau, are concurrent with the reversal of the meridional temperature gradient south of the Tibetan Plateau. He *et al.* (1987) showed that the two stages of the abrupt transitions of the general circulation over Southeast Asia and India are closely related to two similar stages of upper tropospheric warming over the Asian land mass. They also indicated that the rapid warming of the troposphere is recognizable first over the eastern Tibetan Plateau (east of 85°E) , and then over the western Plateau stretching to Iran-Afghanistan (west of 85°E). Yanai *et al.* (1992) revealed that this temperature increase to the east of 85°E is mainly the result of diabatic heating and warm horizontal advection, whereas that to the west of 85°E is caused by adiabatic warming due to large-scale subsidence. Nitta (1983) also found that the heating over the eastern Plateau occurs in a deep tropospheric layer and that the sensible heat flux from the surface is nearly equal to the release of latent heat.

In this section, the seasonal evolution of the temperature field in East Asia, especially over the Tibetan Plateau, is investigated. A useful index of the seasonal (pentadanal) variations in the vertically averaged mean atmospheric temperature is the differential thickness, $\Delta Thick(P)$ defined by,

$$\Delta Thick(P) = Thick(P) - Thick(P-1) \quad (5)$$

$$Thick(P) = Z(200\ \text{hPa}) - Z(500\ \text{hPa}) \quad (6)$$

where Z is height and P is pentad number. Figure 7 shows latitude-time sections of 10-year averaged $\Delta Thick(P)$ averaged between 80°–100°E. In Fig. 7, an increase in thickness is clearly seen until mid-June with an intraseasonal time scale modulation of about 15 days. A notable feature is that the onset phase of the SEAM coincides well with the abrupt increase of thickness over the Tibetan plateau at Pentad 28–29. Matsumoto (1992) showed that remarkable warming of temperature at 300 hPa is recognizable during mid-May over the Tibetan plateau along 30°N between 80°E and 110°E.

To discuss the aforementioned relationships, the spatial distribution of *Thick* (28–29) minus *Thick* (26–27) is presented in Fig. 8. A large positive anomaly in the thickness exists around the Tibetan plateau, implying an increase in the thermal contrast between the Eurasian continent and the surrounding ocean. As a result, it is speculated that the acceleration of low-level monsoon westerlies occurs and finally reaches the South China Sea, causing the onset of the SCSM.

However, here arises a question: why the increases of the thickness before Pentad 28 do not induce the onset of the SEAM? In order to elaborate the seasonal change process of temperature gradient between the Tibetan Plateau and adjacent region, the time section of the temperature contrast be-

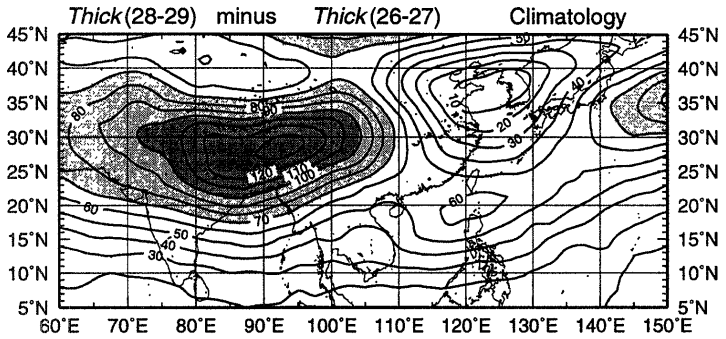

Fig. 8. 10-year averaged thickness between *Thick* (28,29) minus *Thick* (26,27). The contour interval is 10 gpm, with shading (dark shading) indicating regions of differentiated thickness greater than 70 (100 gpm).

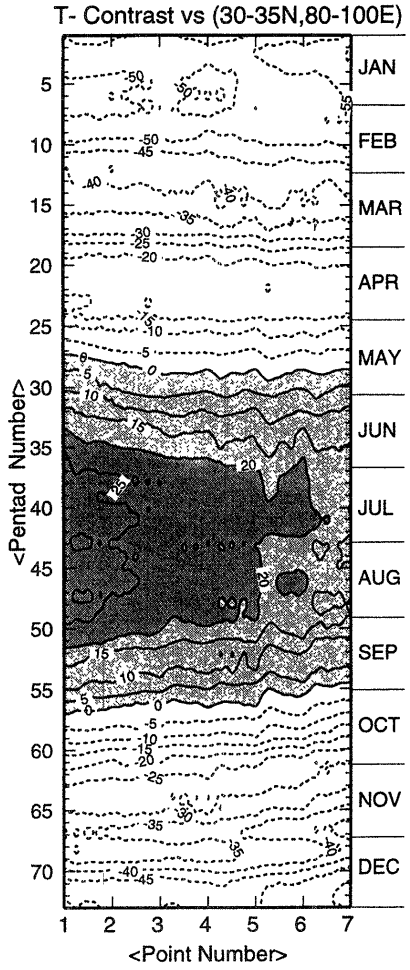

Fig. 9. Time section of temperature contrast between the Tibetan Plateau (30°–35°N, 80°–100°E) and ocean (denoted as bold line in Fig. 10) for climatological mean (1980–89) differential thickness between 200 hPa minus 500 hPa. Light shading denotes between 0 and 20 gpm, while dark shading indicates more than 20 gpm.

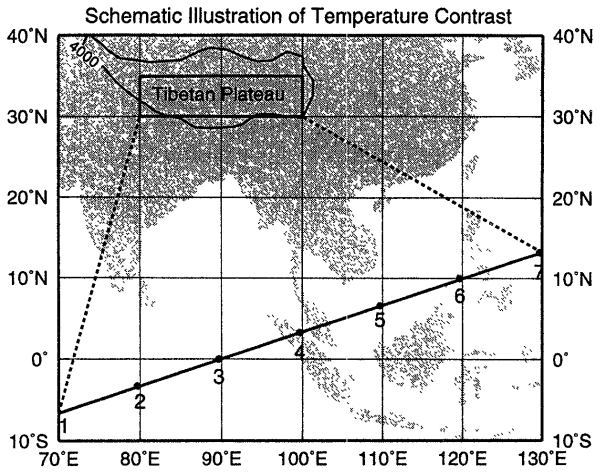

Fig. 10. Schematic illustration of temperature contrast between the Tibetan Plateau and adjacent ocean (shown as bold line with point number). The contour line indicates 4000 m of the sea level altitude. Key region is denoted as solid square (30°–35°N, 80°–100°E).

tween the Tibetan Plateau (30°–35°E, 80°–100°E) and southeastward of the South China Sea and the Bay of Bengal is made in Fig. 9. A schematic illustration of the aforementioned temperature contrast is drawn in Fig. 10. The difference of the temperature is calculated for 200–500 hPa thickness between the Tibetan Plateau (solid square) minus that of the ocean (bold line with point number). In Fig. 9, negative values are seen both before Pentad 28 and after Pentad 57, indicating that mean atmospheric temperature over the Tibetan Plateau is relatively colder than that over the tropics.

On the other hand, positive temperature contrast is found between mid-May and early October. It is interesting to note that the onset of the SEAM is concurrent with the first appearance of the positive temperature contrast in mid-May. In other words,

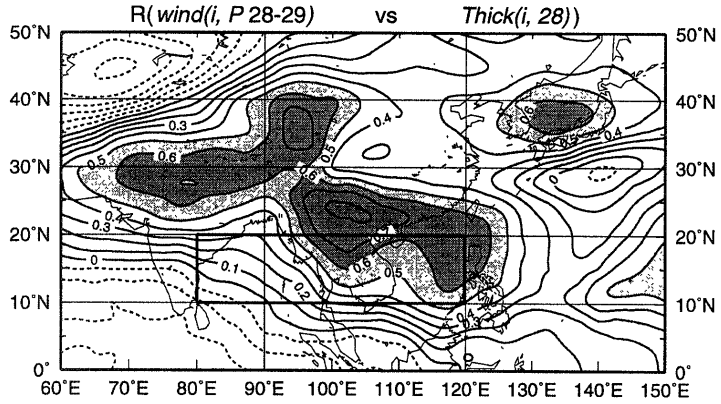

Fig. 11. Spatial distribution of correlation coefficients between interannual variation of wind speed at 850 hPa during Pentad 28, 29 ($wind(i, P28-29)$) over the key region (10°N–20°N, 80°E–120°E) and interannual variation of thickness at Pentad 28 ($Thick(i, 28)$), where i is the year and P is pentad number. Intervals are for 0.1, with shading (dark shading) indicating regions of correlation greater than +0.5 (+0.6).

the increase of temperature at Pentads 22–23 and 25 seen in Fig. 7 is not able to induce the onset of the SCSM.

In this manner, the abrupt warming over the Tibetan Plateau around Pentad 28–29 should occur at the same time as the onset of the SEAM, as is indeed shown in Fig. 7 and Fig. 8. In order to confirm the aforementioned relationship in the interannual variability, the correlation analysis is performed between wind speed at 850 hPa ($wind(i, P28–29)$) over the key region (10°–20°N, 80°–120°E) and $Thick(i, P)$ averaged between 30° and 35°N (Tibetan plateau), where i means interannual variations and P denotes pentad number. The spatial distribution of correlation coefficients between $wind(i, P28\text{-}29)$ and $Thick(i, 28)$ at Pentad 28 is presented in Fig. 11. A positive correlation exists over the Tibetan plateau, which strongly supports the close connection between the warming of the Tibetan plateau and the acceleration of the low-level monsoon westerlies over the key region in the interannual variabilities. In addition, a positive correlation is observed over Japan, which indicates that when the onset of the SCSM occurs then the 200–500 hPa thickness increases over Japan. This high correlation over Japan may result from the propagation of stationary Rossby waves from the South China Sea that are created by tropical heating, which is suggested in Fig. 6. Another feature is that positive correlation is also seen over the Indochina Peninsula, which implies the importance of the warming over the Indochina Peninsula for the commencement of the SEAM. However, the absolute values of increase of the thickness over the Indochina Peninsula seen in Fig. 8 is relatively small compared with that of over the Tibetan Plateau.

5. Conclusions

In previous studies, researchers have suggested that the onset of the SEAM is triggered by intraseasonal variations (*e.g.*, Murakami *et al.*, 1986; Lau *et al.*, 1988; Chen and Chen, 1995; Chen and Weng, 1996) or closely associated with mid-latitude front system (*e.g.*, Chang and Chen, 1995). In particular, we revealed the climatological structure and the mechanism of the abrupt enhancement of the SEAM with regard to atmosphere/land interactions. The main observations of the present study are summarized as follows:

(1) Strong southwesterly monsoon flows in the lower troposphere abruptly enter the west of the Philippines (120°E) from the Bay of Bengal in place of the easterlies during mid-May (Pentad 28: May 16–May 20). The resultant wind anomaly exhibits a cyclonic circulation over the South China Sea, where the slightly enhanced convection is recognizable. In addition, the convection over the Bay of Bengal is much activated during this period.

(2) The warming over the Tibetan plateau increases up to mid-June with the intraseasonal modulation of about 15 day period. It is interesting to note that the commencement of the SEAM and the abrupt increase of warming over the Tibetan plateau occur at the same time, which implies that the onset of the SEAM is closely associated with the meridional temperature gradient between the Tibetan plateau and surrounding regions. This relationship is also confirmed by the correlation analysis between the 200–500 hPa thickness over the Tibetan Plateau and low-level wind over the key region (10°–20°N, 80°–120°E) in the interannual variability.

(3) The cyclonic circulation anomaly and slightly enhanced convection associated with onset of the SCSM plays a role as a vorticity and tropical heat

source, which instigates the propagation of stationary Rossby waves from the South China Sea (low height anomaly) to the northeastward direction around Japan (high height anomaly) and to the Aleutian Islands (low height anomaly). During this period, a distinct singularity of clear skies is observed in Japan (Kawamura and Tian, 1992), which is closely connected with high pressure anomaly associated with the Rossby wave.

These results strongly indicate that the early onset of the summer monsoon over the Bay of Bengal and the South China Sea is induced by an eastward extension of low-level monsoon westerlies up to 120°E during mid-May, which is driven by the continent-ocean thermal contrast enhanced by warming over the Tibetan Plateau.

Acknowledgments

This research has been supported by the Grant-in-Aid for Scientific Research by the Ministry of Education, Science and Culture. Valuable comments on the manuscript were provided by two anonymous reviewers. Special thanks are extended to Dr. Ryuichi Kawamura of National Research Institute for Earth Science and Disaster Prevention for his constant encouragement and helpful advice. We are grateful to Dr. Tetsuo Nakazawa of the Meteorological Research Institute for providing the T_{BB} data from a GMS satellite. Dr. Rikie Suzuki of University of Tsukuba provided rainfall data. Thanks are also due to Dr. Jun Matsumoto for editorial assistance. This research is also funded by Grant-in-Aid 09227208.

References

Chen, T.-C. and J.-M. Chen, 1995: An observational study of the South China Sea monsoon during the 1979 summer: Onset and life cycle. *Mon. Wea. Rev.*, **123**, 2295–2318.

Chen, T.-C. and K. Takahashi, 1994: Diurnal variation of outgoing longwave radiation in the vicinity of the South China Sea: Effect of intraseasonal oscillation. *Mon. Wea. Rev.*, **123**, 566–577.

Chen, T.-C., M.-C. Yen and M. Murakami, 1988: The water vapor transport associated with the 30–50-day oscillation over the Asian monsoon regions during 1979 summer. *Mon. Wea. Rev.*, **116**, 1983–2002.

Chen, T.-C. and S.-P. Weng, 1996: Some effects of intraseasonal oscillation on the equatorial waves over the western tropical Pacific-South China Sea region during the Northern Summer. *Mon. Wea. Rev.*, **124**, 751–756.

Fu, C. and J.O. Fletcher, 1985: The relationship between Tibet-tropical ocean thermal contrast and interannual variability of Indian monsoon rainfall. *J. Climate Appl. Meteor.*, **24**, 841–847.

Gao, Y.-X., M.-C. Tang, S.-W. Luo, Z.-B. Shen and C. Li, 1981: Some aspects of recent research on the Qinghai-Xizang Plateau meteorology. *Bull. Amer. Meteor. Soc.*, **62**, 31–35.

Chang C.-P. and G.T.-J. Chen, 1995: Tropical circulations associated with southwest monsoon onset and westerly surges over the South China Sea. *Mon. Wea. Rev.*, **123**, 3254–3267.

He, H., J.W. McGinnis, Z. Song and M. Yanai, 1987: Onset of the Asian monsoon in 1979 and the effect of the Tibetan Plateau. *Mon. Wea. Rev.*, **115**, 1966–1995.

Hirasawa, N., K. Kato and T. Takeda, 1995: Abrupt change in the characteristics of the cloud zone in subtropical East Asia around the middle of May. *J. Meteor. Soc. Japan*, **73**, 221–239.

Kawamura, R. and S.-F. Tian, 1992: Singularity in Japan and teleconnection patterns appearing in 500 hPa geopotential height field of the Northern Hemisphere. *Tenki*, **39**, 75–85 (in Japanese).

Khromov, S.P., 1957: Die geographische Verbreitung der Monsune. *Petermanns Geogr. Mitt.*, **101**, 234–237.

Krishnamurti, T.N., P. Ardanuy, Y. Ramanathan and R. Pasch, 1981: On the onset vortex of the summer monsoon. *Mon. Wea. Rev.*, **109**. 344–363.

Lau, K.-M., G.J. Yang and S.H. Shen, 1988: Seasonal and intraseasonal climatology of summer monsoon rainfall over East Asia. *Mon. Wea. Rev.*, **116**, 18–37.

Lau, K.M. and S. Yang, 1996: Seasonal variation, abrupt transition, and intraseasonal variability associated with the Asian summer monsoon in the GLA GCM. *J. Climate*, **9**, 965–985.

Li, C. and M. Yanai, 1996: The onset and interannual variability of the Asian summer monsoon in relation to land-sea thermal contrast. *J. Climate*, **9**, 358–375.

Luo, H. and M. Yanai, 1984: The large-scale circulation and heat sources over the Tibetan Plateau and surrounding areas during the early summer of 1979. Part II: Heat and moisture budgets. *Mon. Wea. Rev.*, **112**, 966–989.

Matsumoto, J., 1992: The seasonal changes in Asian and Australian monsoon regions. *J. Meteor. Soc. Japan*, **70**, 257–273.

Matsumoto, J., 1997: Seasonal transition of summer rainy season over Indochina and adjacent monsoon region. *Advances in Atmospheric Sciences*, **14**, 231–245.

Murakami, M., 1983: Analysis of the deep convective activity over the western Pacific and Southeast Asia. Part I: Diurnal variation. *J. Meteor. Soc. Japan*, **61**, 60–77.

Murakami, T. and T. Nakazawa, 1985: Transition from the Southern to Northern Hemisphere summer monsoon. *Mon. Wea. Rev.*, **113**, 1470–1486.

Murakami, T. and L.X. Chen and A. Xie, 1986: Relationship among seasonal cycles, low-f requency oscillations, and transient disturbances as revealed from outgoing longwave radiation data. *Mon. Wea. Rev.*, **114**, 1456–1465.

Murakami, T., 1987: Effects of the Tibetan Plateau. *Monsoon Meteorology*, C.-P. Chang and T.N. Krishnamurti, Eds., Oxford University Press, 26–59.

Murakami, T., 1993: Nature of monsoon Asia. *Kagaku*, **63**, 619–625 (in Japanese).

Murakami, T. and J. Matsumoto, 1994: Summer monsoon over the Asian continent and western North Pa-

cific. *J. Meteor. Soc. Japan*, **72**, 719–745.
Nakazawa, T., 1992: Seasonal phase lock of intraseasonal variation during the Asian summer monsoon. *J. Meteor. Soc. Japan*, **70**, 597–611.
National Climatic Data Center, 1994: Global daily summary (CD-Rom.).
Nitta, Ts., 1983: Observational study of heat sources over the eastern Tibetan Plateau during the summer monsoon. *J. Meteor. Soc. Japan*, **61**, 590–605.
Nitta, Ts., 1986: Long-term variations of cloud amount in the western Pacific region. *J. Meteor. Soc. Japan*, **64**, 373–390.
Nitta, Ts., 1987: Convective activities in the tropical western Pacific and their impact on the Northern Hemisphere summer circulation. *J. Meteor. Soc. Japan*, **65**, 373–390.
So C.H. and J.C.L. Chan, 1997: An observational study on the onset of the summer monsoon over South China around Hong Kong., *J. Meteor. Soc. Japan*, **75**, 43–57.
Tanaka, M., 1992: Intraseasonal oscillation and the onset and retreat dates of the summer monsoon over East, Southeast Asia and the western Pacific region using GMS high cloud amount data. *J. Meteor. Soc. Japan*, *70*, 613–629
Ueda, H., T. Yasunari and R. Kawamura, 1995: Abrupt seasonal change of large-scale convective activity over the western Pacific in the northern summer. *J. Meteor. Soc. Japan*, **73**, 795–809.
Ueda, H. and T. Yasunari, 1996: Maturing process of summer monsoon over the western North Pacific - A coupled Ocean/Atmosphere system. *J. Meteor. Soc. Japan*, **74**, 493–508.
Ueda, H. and T. Yasunari, 1997: Relationships Between Seasonal Evolution of Oceanic Monsoon over the Western Pacific and Summer Weather Regimes around Japan -A Case Study of Severely Cool/Hot Summer Years of 1993/94-. *Tenki* (accepted).
Yanai, M., C. Li. and Z. Song, 1992: Seasonal heating of the Tibetan Plateau and its effects on the evolution of the Asian summer monsoon. *J. Meteor. Soc. Japan*, **70**, 319–351.
Wang, B. and X. Xu, 1997: Northern Hemisphere summer singularities and climatological intraseasonal oscillation. *J. Climate*, **10**, 1071–1085.

ベンガル湾及び南シナ海上の夏季モンスーンの早期開始における チベット高原の温度上昇の役割

植田宏昭[1]・安成哲三
（筑波大学地球科学系）

本研究ではベンガル湾及び南シナ海上の東南アジアモンスーン（SEAM）の開始のメカニズムを、チベット高原とその周囲の海洋との温度コントラストの視点から調べた。循環場の解析にはECMWFによる5日平均客観解析データ（1980–1989年）、対流活動の指標としてはGMSの5日平均等価黒体温度（TBB）データ（1980–1994年）を用いた。東南アジアモンスーンのいち早い開始は、第28半旬（5月16–20日）に下層のモンスーン西風気流の加速を伴って見られ、その後6月の上旬に2回目のモンスーン強化が生じている。

春から夏にかけてのチベット高原上では、200–500 hPaの気層の温度上昇が約15日間隔で上昇している。特に5月中旬のチベット高原上の温度上昇は、SEAMの開始と一致している点が重要である。すなわちチベット高原とその周囲の海洋との温度差異は、下層のモンスーン気流の加速と東方への拡大を引き起こし、結果として南シナ海モンスーン（SCSM）を含むSEAMの急激な開始をもたらす。この関係は、（10°–20°N, 80°–120°E）での下層の風と200–500 hPaの層厚との年々変動の相関解析によっても確認された。

中緯度への影響としては、SCSMの開始による低気圧性渦度と熱源により、定常ロスビー波が南シナ海上で励起され、更に北東方向に伝播している。この波の下流の日本付近は正の高度場偏差が現われ、川村と田（1992）が示した5月中旬の日本の晴天の特異日と一致している。

[1]日本学術振興会特別研究員